Structural Engineering and Mechanics, *Vol. 69, No. 4 (2019) 417-426*
DOI: https://doi.org/10.12989/sem.2019.69.4.417

Study of buckling stability of cracked plates under uniaxial compression using singular FEM

Sina Saberi[1a], Parham Memarzadeh[1b] and Tadeh Zirakian*[2]

[1]Department of Civil Engineering, Najafabad Branch, Islamic Azad University, P.O. Box 85141-43131, Najafabad, Iran
[2]Department of Civil Engineering and Construction Management, California State University, Northridge, CA, USA

(Received July 17, 2018, Revised December 31, 2018, Accepted January 13, 2019)

Abstract. Buckling is one of the major causes of failure in thin-walled plate members and the presence of cracks with different lengths and locations in such structures may adversely affect this phenomenon. This study focuses on the buckling stability assessment of centrally and non-centrally cracked plates with small-, intermediate-, and large-size cracks, and different aspect ratios as well as support conditions, subjected to uniaxial compression. To this end, numerical models of the cracked plates were created through singular finite element method using a computational code developed in MATLAB. Eigen-buckling analyses were also performed to study the stability behavior of the plates. The numerical results and findings of this research demonstrate the effectiveness of the crack length and location on the buckling capacity of thin plates; however, the degree of efficacy of these parameters in plates with various aspect ratios and support conditions is found to be significantly different. Overall, careful consideration of the aspect ratio, support conditions, and crack parameters in buckling analysis of plates is crucial for efficient stability design and successful application of such thin-walled members.

Keywords: thin-walled structures; plates; crack; buckling; numerical simulation

1. Introduction

Buckling of thin-walled structures is one of the most important problems which should be considered in structural design. Thin plates as basic structural elements, which are commonly used in practical applications, have the potential to being subjected to buckling phenomenon. Such structural elements are vulnerable to different types of defects such as cracks. Such defects can affect the buckling coefficient and bearing capacity of thin plates. Hence, it is important to study and understand the buckling behavior of cracked plates and evaluate the impact of the effective parameters. For instance, systematic analytical and experimental studies have been recently performed and reported by Ghanbari Ghazijahani and his co-researchers, e.g. Ghanbari Ghazijahani *et al.* (2014, 2015, 2016), on the structural behavior and buckling stability of a series of thin-walled members, viz. steel cylindrical shells, truncated cones, and circular tubes, with dent-shaped defects which has been quite helpful and inspiring in understanding and quantifying the effects of dent imperfections.

In this regard, some studies have been conducted on buckling behaviors of centrally and/or edge cracked plates. Markström and StoÅkers (1980), Sih and Lee (1986), Shaw and Huang (1990), Agnihotri (1993), Guz and Dyshel (2001, 2002), Vafai *et al.* (2002), Brighenti (2005a, b), and Seifi and Khoda-yari (2011) investigated the effects of different crack parameters on buckling behavior of tensioned plates with various boundary conditions. It was demonstrated that the compressive stresses around the crack can cause the plate buckling, even when the plate is under tension. Furthermore, in studies carried out by Sih and Lee (1986), Brighenti (2005a, b), Pan *et al.* (2013), Sadek and Tawfik (2016), Seif and Kabir (2017), and Shi *et al.* (2017), the buckling behavior of cracked plates under compression was evaluated. Their investigations showed that the behavior of a cracked plate can be different depending upon the location of the crack being either in the center or in the edge of the plate. Also, it was indicated that the effect of boundary conditions on the buckling load is inconsiderable for plates with small cracks, while it can be noticeable for those with large cracks. Additionally, Shahverdi and Navardi (2017) developed an elemental approach based on the differential quadrature method for free vibration analysis of cracked thin plate structures. The agreement between the results of the proposed method and those found by finite element method was reported to be good.

Considering the possible effectiveness of cracks on the buckling stability of thin plates, some studies have also been reported on the repair of such cracked thin-walled members. Jamal-Omidi *et al.* (2014) examined the fracture behavior of centrally cracked aluminum plates repaired with composite patches using extended finite element method. The effects of crack lengths, patch materials, orientation of plies, adhesive and patch thickness were investigated to estimate the stress intensity factor at the crack tip. In another study, Bouchiba and Serier (2016) developed an

*Corresponding author, Ph.D.
E-mail: tadeh.zirakian@csun.edu
[a]M.Sc.
E-mail: saberi.sina@hotmail.com
[b]Ph.D.
E-mail: p-memar@iaun.ac.ir

http://www.techno-press.com/journals/sem&subpage=7
ISSN: 1225-4568 (Print), 1598-6217 (Online)

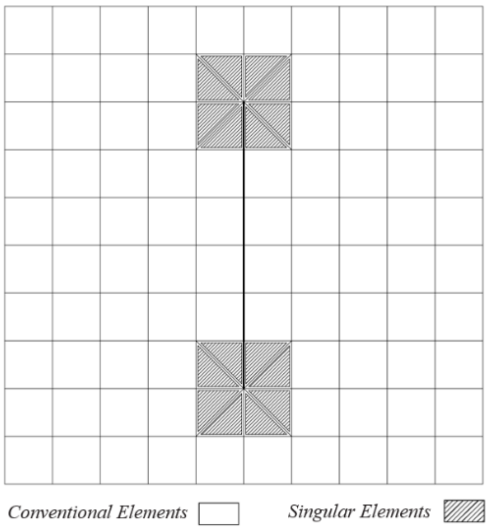

Fig. 1 Details of modeling of a cracked plate using singular and conventional finite elements

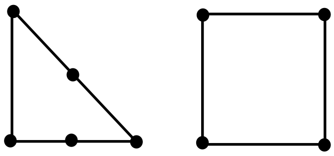

Fig. 2 Details of in-plane triangular and quadrilateral elements

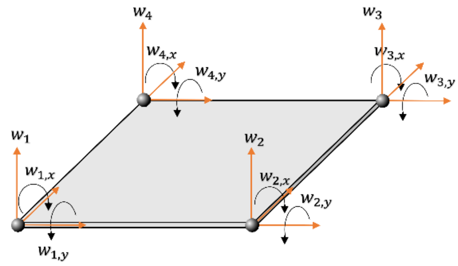

(a) Conventional

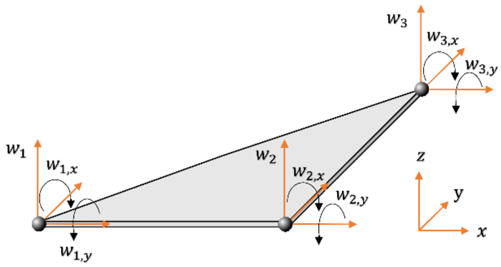

(b) Singular

Fig. 3 Details of out-of-plane elements

optimization method of patch shape in order to improve repair of cracked plates. As a result, families of optimal shapes with specific geometric features around the crack tip and at the horizontal end of the patch were identified.

A crack in a plate element may be generally observed at any location. Thus, evaluation of the effectiveness of crack location is essential for gaining a better understanding of the stability behavior of cracked plates. The problem of buckling behavior of non-centrally cracked plates has not been adequately investigated by researchers. Among the few reported research endeavors, the study performed by Khedmati *et al.* (2009) is noted herein. This work was limited to the study of the buckling of simply supported cracked plates subjected to compressive load. It was shown that the size and location of cracks can have significant effects on the buckling capacity of such thin-walled structures.

This study intends to extend the previous research on the compressed cracked plates to those with various boundary conditions, aspect ratios, and crack lengths as well as locations. To this end, eigen-buckling equations of the cracked plates are implemented in MATLAB software environment and analyzed by using Singular Finite Element Method (SFEM). Following the comparison of the results of this study with those reported in reliable references and verification of the validity of the models, detailed investigations have been made and discussed in the paper.

2. Conventional and singular finite elements

In this research, numerical modeling of the cracked plates is performed by using the conventional finite elements except for areas around the crack tips where singular elements are used. Singular elements are capable of simulating the singularity of stresses near the crack tips. Figs. 1 and 2 show a cracked plate modeling details as well as the five-noded singular and four-noded conventional elements with triangular and quadrilateral shapes used for in-plane analyses, respectively. More details on the properties of these elements can be found in Stren (1979).

The properties of the out-of-plane four-noded conventional and three-noded singular elements with three degrees of freedom at each node including a transverse deflection and two rotations are illustrated in Fig. 3.

The transverse deflection, w, can be expressed in polar coordinate system and in matrix form using Eqs. (1) and (2), respectively (Khedmati *et al.* 2009).

$$\begin{aligned} w = {} & \alpha_1 + \alpha_2\, r\cos\theta + \alpha_3\, r\sin\theta + \alpha_4\, r^{\frac{3}{2}}\cos\left(\frac{\theta}{2}\right) \\ & + \alpha_5 r^{\frac{3}{2}}\sin\left(\frac{\theta}{2}\right) \\ & + \alpha_6\, r^{\frac{3}{2}}\left(cos^3\left(\frac{\theta}{2}\right) + sin^3\left(\frac{\theta}{2}\right)\right) \\ & + \alpha_7\, r^2\sin\theta\cos\theta + \alpha_8\, r^2\cos^2\theta \\ & + \alpha_9\, r^2 sin^2\theta \end{aligned} \tag{1}$$

$$w = [\varphi]\,\{\alpha\} \tag{2}$$

In Eq. (2), $\{\alpha\}$ is the vector of the unknowns and $[\varphi]$ is the matrix of the interpolation functions defined as follows

$$[\varphi] = \left[\begin{matrix} 1 & r\cos\theta & r\sin\theta & r^{\frac{3}{2}}cos\left(\frac{\theta}{2}\right) & \cdots & r^2 sin^2\,\theta \end{matrix}\right] \tag{3}$$

To connect the singular element with a conventional element, one should follow the standard FEM formulation to exchange $\{\alpha\}$ for nodal degrees of freedom. Using the transverse deflection (Eq. (1)), the following equation can be obtained

$$\begin{Bmatrix} w \\ w_{,x} \\ w_{,y} \end{Bmatrix} = [B]\,\{\alpha\} \tag{4}$$

where, comma denotes partial differentiation with respect to the geometric variables x and y. After substituting the nodal coordinates into Eq. (4), the following relation between the parameters $\{\alpha\}$ and nodal degrees of freedom $\{\delta_e\}$ can be obtained

$$\{\delta_e\} = [C]\,\{\alpha\} \tag{5}$$

where, $[C]$ is the corresponding transformation matrix. The transverse deflection may then be expressed as

$$w = [\varphi]\,[C]^{-1}\,\{\delta_e\} \tag{6}$$

The shape function matrix $[\Phi]$ can be consequently derived as

$$[\Phi] = [\varphi]\,[C]^{-1} \tag{7}$$

Finally, the transverse deflections near the crack tips may be determined using the following equation

$$w = [\Phi]\,\{\delta_e\} \tag{8}$$

Further details on the shape functions used for the out-of-plane analysis of the conventional quadrilateral elements can be found in (Reddy 2006).

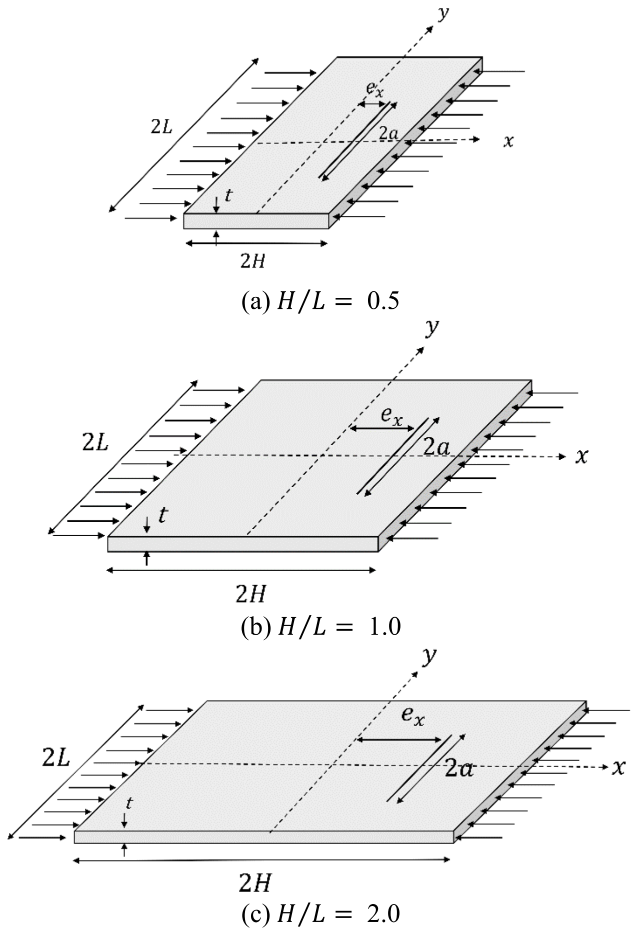

Fig. 4 Cracked plates with different aspect ratios

3. Formulation

The finite element formulation for the present method is based on Von Karman's linearized theory for buckling of plates subjected to pre-buckling state of plane stresses. The total potential energy for a thin plate element under the action of in-plane forces and out-of-plane deflections is defined as follows

$$\Pi = U + V \tag{9}$$

where, U and V are the element strain energy due to bending and the potentials from external mechanical loads, respectively, which can be written as

$$\begin{aligned} \mathrm{U} = \int_A \{D\big[w_{,xx}^2 + 2\nu\, w_{,xx}\, w_{,yy} + w_{,yy}^2 \\ + 2(1-\nu) w_{,xy}^2\big]\}\, dA \end{aligned} \tag{10}$$

$$V = \int_A \left[N_x\, w_{,x}^2 + 2N_{xy}\, w_{,x}\, w_{,y} + N_y\, w_{,y}^2 \right] dA \tag{11}$$

In these equations, N_x, N_{xy}, and N_y are the in-plane forces per unit length of plate boundary in the corresponding directions, and D is the plate flexural rigidity, defined as

$$D = \frac{E\,t^3}{12(1-\nu^2)} \begin{bmatrix} 1 & \nu & 0 \\ \nu & 1 & 0 \\ 0 & 0 & \dfrac{(1-\nu)}{2} \end{bmatrix} \tag{12}$$

in which, E and ν are the Young's modulus and Poisson's ratio of material, respectively. This numerical study is performed by the aid of a standard finite element code developed in MATLAB software. Based on the principle of minimum total potential energy, the equilibrium equations are obtained from variation of Eq. (9)

$$\delta\Pi = \delta U + \delta V = 0 \tag{13}$$

where

$$\delta\Pi = [K_s]\{\delta W\}^T + \left[K_g\right]\{\delta W\}^T = 0 \tag{14}$$

In Eq. (14), $[K_s]$ is the standard stiffness matrix and $\left[K_g\right]$ is the geometric stiffness matrix due to the in-plane stresses.

Ultimately, the calculation of the Eulerian buckling load is based on the following eigenvalue problem

$$([K_s] - \lambda_i\,[K_g])\,\{\beta_i\} = \{0\} \tag{15}$$

where, λ_i is the eigenvalue and $\{\beta_i\}$ is the plate buckling mode-shape (eigen) vector. Usually, the lowest value of λ_i is of interest which is denoted as λ_{cr}. The value of the plate

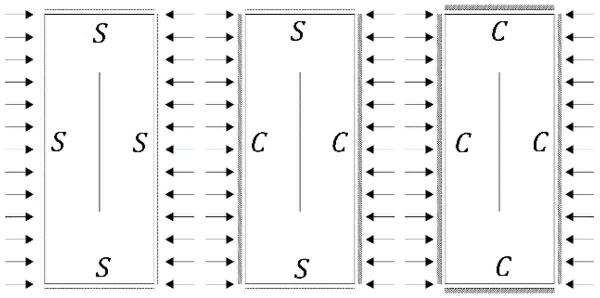

Fig. 5 Boundary conditions of cracked plates; *SS* (left), *CS* (center), *CC* (right)

Table 1 Considered plate aspect ratios and crack locations as well as lengths

H/L	e_x/H	a/L					
0.5	0.00	0	0.11	0.22	0.33	0.44	0.55
			0.66	0.77	0.88	0.94	
	0.20	0	0.11	0.22	0.33	0.44	0.55
			0.66	0.77	0.88	0.94	
	0.40	0	0.11	0.22	0.33	0.44	0.55
			0.66	0.77	0.88	0.94	
	0.60	0	0.11	0.22	0.33	0.44	0.55
			0.66	0.77	0.88	0.94	
	0.80	0	0.11	0.22	0.33	0.44	0.55
			0.66	0.77	0.88	0.94	
1.0	0.00	0	0.1	0.2	0.3	0.4	0.5
			0.6	0.7	0.8	0.9	
	0.14	0	0.1	0.2	0.3	0.4	0.5
			0.6	0.7	0.8	0.9	
	0.27	0	0.1	0.2	0.3	0.4	0.5
			0.6	0.7	0.8	0.9	
	0.41	0	0.1	0.2	0.3	0.4	0.5
			0.6	0.7	0.8	0.9	
	0.55	0	0.1	0.2	0.3	0.4	0.5
			0.6	0.7	0.8	0.9	
	0.68	0	0.1	0.2	0.3	0.4	0.5
			0.6	0.7	0.8	0.9	
	0.86	0	0.1	0.2	0.3	0.4	0.5
			0.6	0.7	0.8	0.9	
2.0	0.00	0	0.1	0.2	0.3	0.4	0.5
			0.6	0.7	0.8	0.9	
	0.22	0	0.1	0.2	0.3	0.4	0.5
			0.6	0.7	0.8	0.9	
	0.45	0	0.1	0.2	0.3	0.4	0.5
			0.6	0.7	0.8	0.9	
	0.68	0	0.1	0.2	0.3	0.4	0.5
			0.6	0.7	0.8	0.9	
	0.90	0	0.1	0.2	0.3	0.4	0.5
			0.6	0.7	0.8	0.9	

buckling coefficient can be obtained using the following equation where L denotes half plate length.

$$k = \left(\frac{\lambda_{cr}\,(2L)^2}{\pi^2 D}\right) \tag{16}$$

4. Model description

The parameters under study are the plate aspect ratio, boundary conditions, and crack length as well as location. Fig. 4 shows the plates with three 0.5, 1.0, and 2.0 aspect

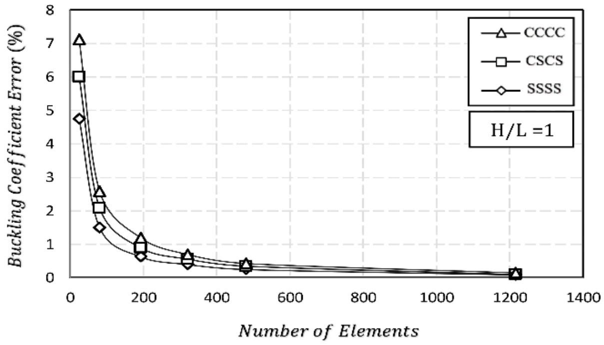

Fig. 6 Sensitivity of un-cracked plate to mesh size (for exact values refer to Timoshenko and Gere (1961))

Table 2 Comparison of results for un-cracked plate with $H/L = 1.0$

Buckling coefficient	Timoshenko and Gere (1961)	This study
k_{ss}	4.00	3.9964
k_{cs}	6.74	6.7338
k_{cc}	10.07	10.0555

Table 3 Comparison of results for cracked plate with $H/L = 2.0$

Buckling coefficient	a/L	Brighenti (2005a)	Khedmati *et al.* (2009)	This study
k_{ss}	0.1	4.0242	4.0248	4.0123
	0.2	4.0915	4.1043	4.0761
	0.3	4.1923	4.2123	4.1678
	0.4	4.2922	4.3434	4.2666
	0.5	4.3885	4.4725	4.3568

ratios (H/L). In this figure, $2a$ is the crack length, t is the plate thickness, and location of the crack is expressed by the crack distance ratio parameter (e_x/H). e_x is the distance between the central y-axis of the plate and the crack, as depicted in Fig. 4.

As shown in Fig. 5, three types of support conditions are considered in this study, which include: (a) all plate edges simply supported (*SS*), (b) two loaded edges clamped and the two others simply supported (*CS*), and (c) all plate edges clamped (*CC*).

The considered crack length ratios (a/L) for plates with different aspect ratios and crack locations are also summarized in Table 1.

Consistent with all cracked plate models, the following assumptions are made for geometrical and material properties: $2L = 1200$ mm, $t = 10$ mm, $E = 1\times10^6$ MPa, and $\nu = 0.3$.

5. Model verification

In order to investigate the convergence of the numerical results, some sensitivity analyses are performed on both un-cracked and cracked plates. Fig. 6 shows the sensitivity of the models to various mesh sizes of the un-cracked plate.

Table 4 Crack categories based on crack length

Crack size	Small	Intermediate	Large
a/L	< 0.5	0.5 – 0.75	> 0.75

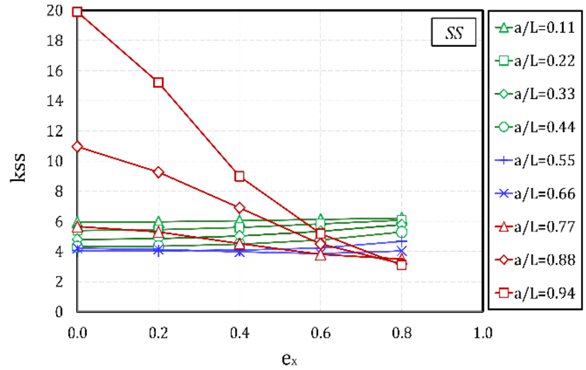

(a) *SS*

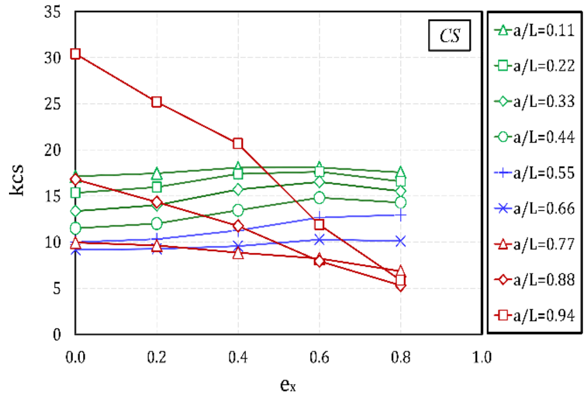

(b) *CS*

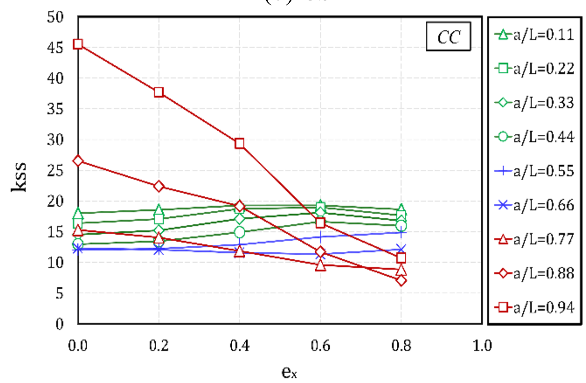

(c) *CC*

Fig. 7 Effect of crack location on critical buckling coefficient of plates with $H/L = 0.5$

Similar studies are performed on various cracked plates; nonetheless, the results for the un-cracked plates are only presented herein for brevity. Based on the results obtained from the sensitivity analyses, a mesh of 40×40 mm for each element is chosen.

Furthermore, another sensitivity study is carried out for choosing the appropriate number of Gauss points which are necessary for numerical integration of Eqs. (15) and (16). As a consequence, 9 (3×3) and 36 (6×6) Gauss points are chosen for numerical integration of the conventional and singular elements, respectively, for both in-plane and out-

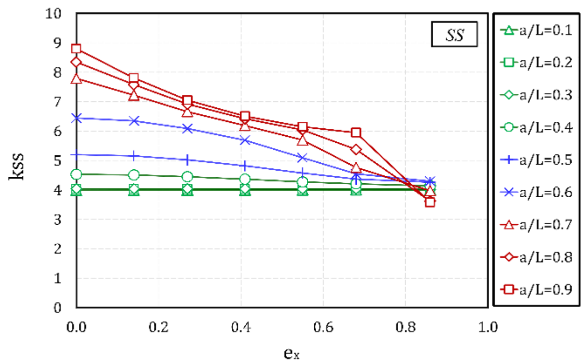

(a) *SS*

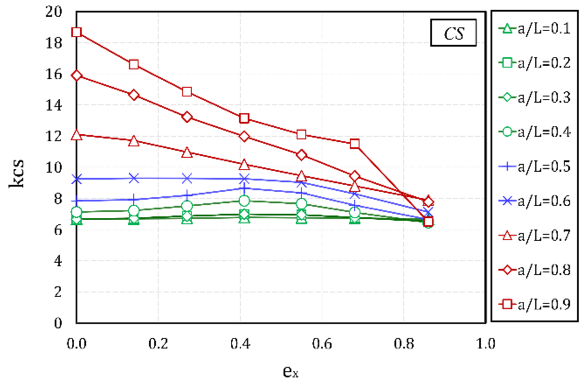

(b) *CS*

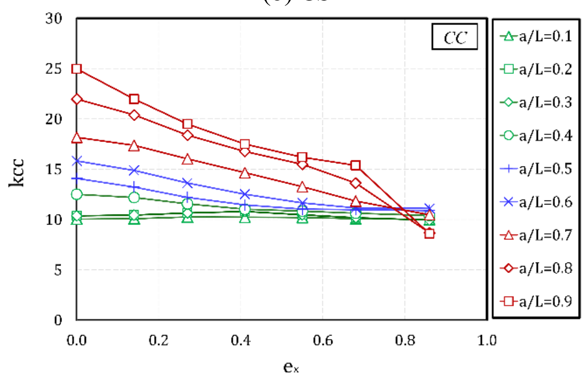

(c) *CC*

Fig. 8 Effect of crack location on critical buckling coefficient of plates with $H/L = 1.0$

of-plane analyses.

For validation of the numerical models, un-cracked and cracked plates are analyzed using the developed MATLAB code. Tables 2 and 3 show the comparison of the results of this study and those reported in reliable references for un-cracked and cracked plate models, respectively. From the tables, the agreement between the results is quite satisfactory.

6. Discussion of results

In this section, the effects of the considered parameters, viz. plate aspect ratio, support conditions, and crack size as well as location, on the buckling coefficient are investigated on the basis rof the results from numerical analyses. It is

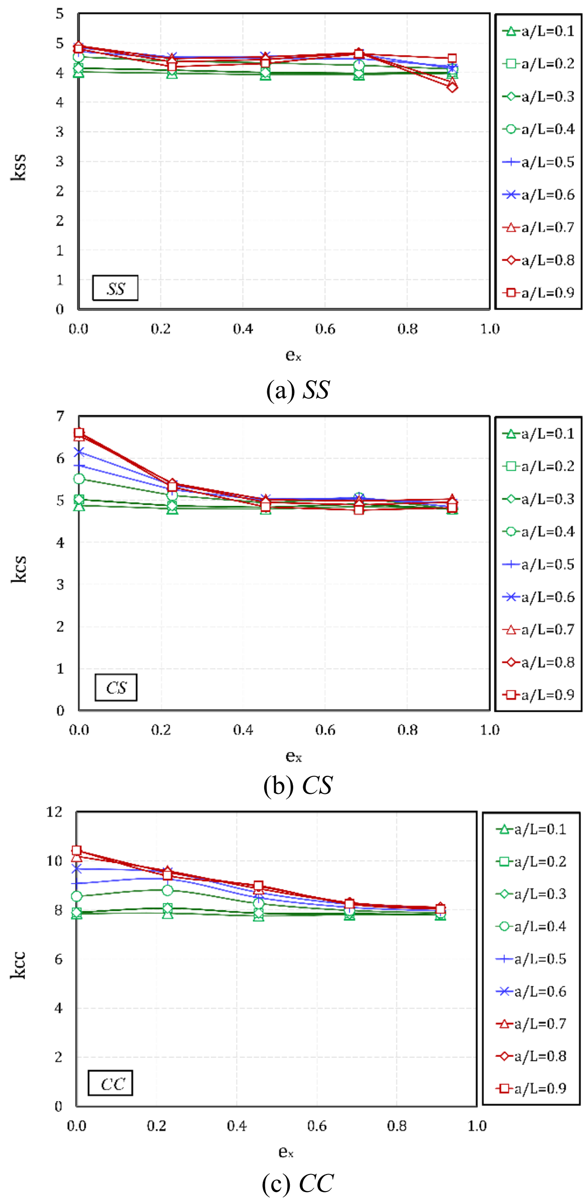

Fig. 9 Effect of crack location on critical buckling coefficient of plates with $H/L = 2.0$

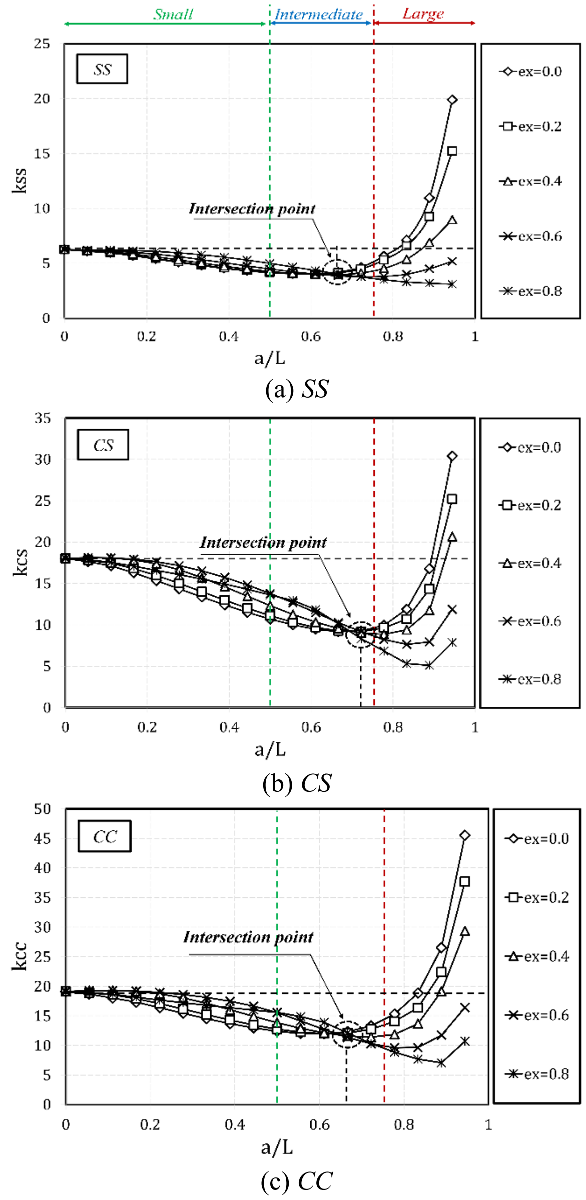

Fig. 10 Effect of crack length on critical buckling coefficient of plates with $H/L = 0.5$

reiterated that the results discussed in the subsequent sections were obtained from developing numerical models based on SFEM and also performing eigen-value buckling analyses.

6.1 Effect of crack location

Figs. 7, 8, and 9 illustrate the buckling coefficients of the cracked plates with different supports vs. the parameter of crack location for plate aspect ratios 0.5, 1.0, and 2.0, respectively. In order for better understanding the behavior of the cracked plates, the cracks are classified into three categories: small, intermediate, and large, as defined in Table 4.

As shown in Figs. 7, 8, and 9, in case of the large cracks the buckling coefficient of non-centrally cracked plate is less than that of the corresponding centrally cracked plate. In other words, increase of crack distance ratio (e_x/H) results in decrease of buckling coefficient. This result is observed for plates with different aspect ratios and boundary conditions. The mean values for reduction of the buckling coefficient due to increase of the crack distance from the plate center are approximately 60%, 50%, and 20% with the standard deviations around 20%, 11%, and 8% for the plates having aspect ratios 0.5, 1.0, and 2.0, respectively.

In the case of small cracks, the behavior of the plates is different, depending on the plate aspect ratio. For plates with aspect ratio 0.5, increase of the distance ratio (e_x/H) augments the buckling coefficient by an average of about 17%, while for plates with aspect ratio 2.0, increase of the distance of small cracks from the plate center lowers the buckling coefficient by about 4% on average. For the case of plates with aspect ratio 1.0, the buckling coefficient of

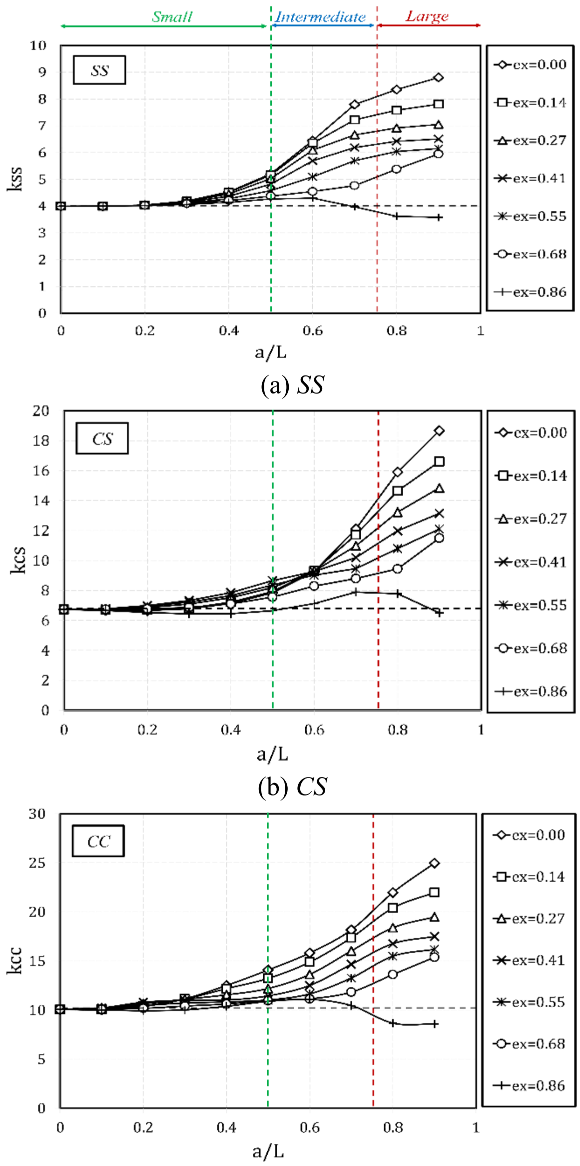

(a) *SS*

(b) *CS*

(c) *CC*

Fig. 11 Effect of crack length on critical buckling coefficient of plates with $H/L = 1.0$

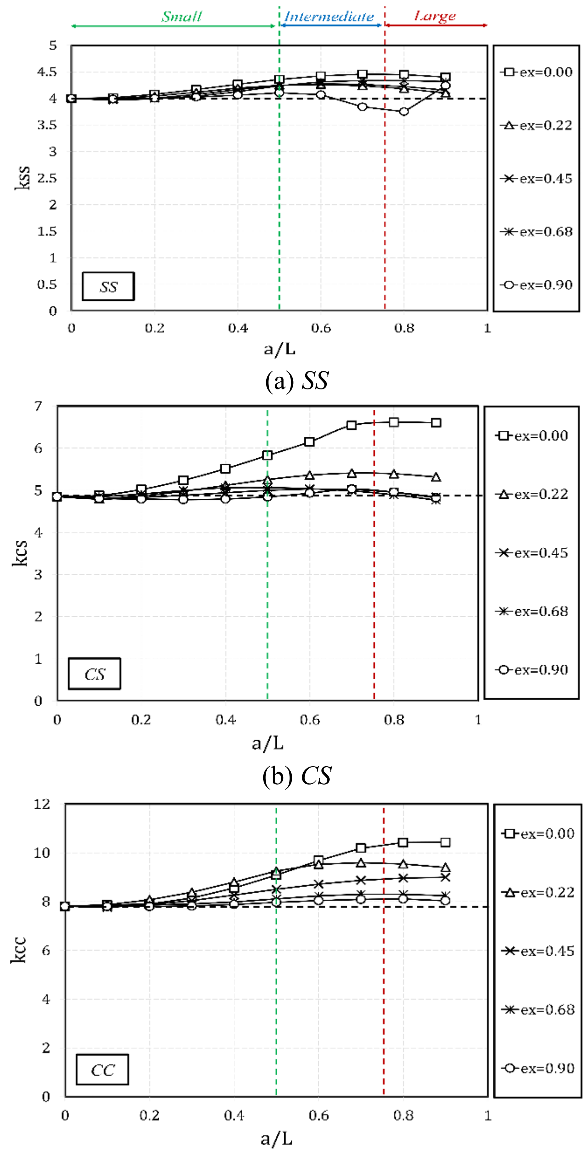

(a) *SS*

(b) *CS*

(c) *CC*

Fig. 12 Effect of crack length on critical buckling coefficient of plates with $H/L = 2.0$

the non-centrally cracked plate remains fairly constant with the variation of the crack location. From the figures, there is scatter in results for the cracks with intermediate lengths and no particular trend is identified for the variation of the buckling coefficient with respect to the crack location.

6.2 Effect of crack length

Figs. 10, 11, and 12 show the buckling coefficients of the cracked plates with different supports plotted against the parameter of crack length (a/L) for respective 0.5, 1.0, and 2.0 aspect ratios. It is observed that for plates with aspect ratios 1.0 and 2.0 increase of the crack length results in the increase of the buckling coefficient for the range of small cracks, while an opposite trend is seen for plates with aspect ratio 0.5 where increase of the crack size results in decrease of the coefficient for the range of small and intermediate cracks. As well, from Fig. 10 it is evident that for plates with aspect ratio 0.5 the curves intersect at a point corresponding to a/L ratio of about 0.7. This indicates that at this specific point the crack location has negligible effect on the buckling coefficient.

In addition, from the figures, the existence of a large crack in the plate may increase or decrease the buckling coefficient depending on the crack length and location. Moreover, dispersion of the curves in the region for large cracks is indicative of higher sensitivity of the buckling coefficient to the crack location in this range than for the cases of the small and intermediate cracks.

6.3 Effect of boundary conditions

Fig. 13 shows the plots of average critical buckling coefficients versus crack length ratio (a/L) for *SS*, *CS*, and *CC* support conditions and 0.5, 1.0, and 2.0 plate aspect ratios.

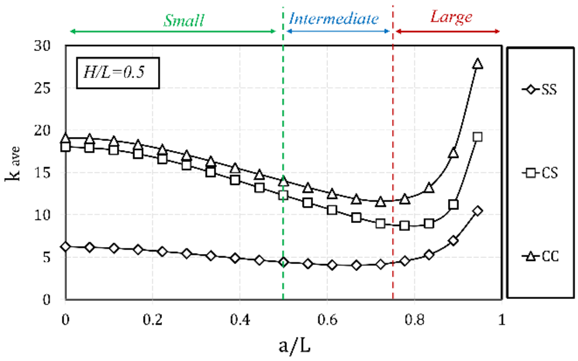

(a) $H/L = 0.5$

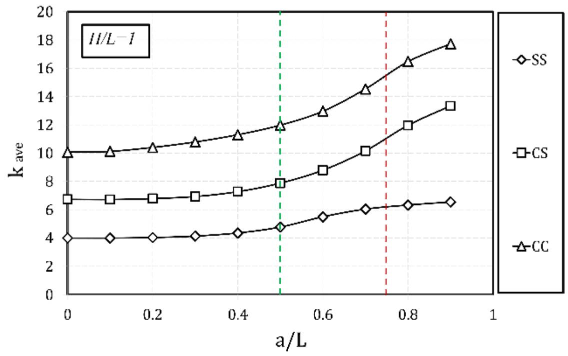

(b) $H/L = 1.0$

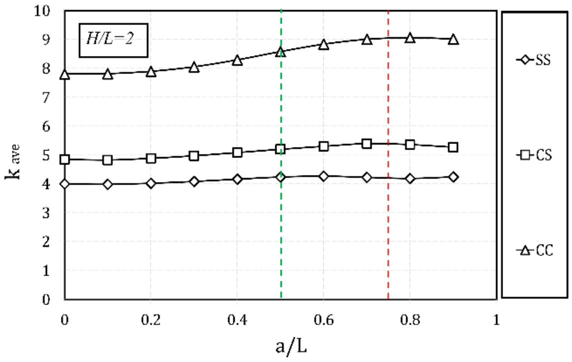

(c) $H/L = 2.0$

Fig. 13 Effect of support conditions on critical buckling coefficient of plates with different aspect ratios

From Figs. 13(a), 13(b) and 13(c) it is found that for plates with small cracks the fixity of the loading edges is highly effective on the buckling coefficient. Consistent with all aspect ratios, the highest and the lowest buckling coefficient values are attributed to *CC* and *SS* support conditions, respectively. Also, it is noted that the buckling coefficients have the highest values for the smallest aspect ratio, i.e., 0.5, while these values decrease as the plate aspect ratio increases from 0.5 to 2.0. This is attributed to the fact that the ratio of the clamped to total boundary lengths is greater for plates with smaller aspect ratios.

7. Discussion on the effectiveness of the buckling modes

For further discussion, the buckling coefficient-crack location curve for $a/L = 0.9$, depicted in Fig. 8(a), is re-

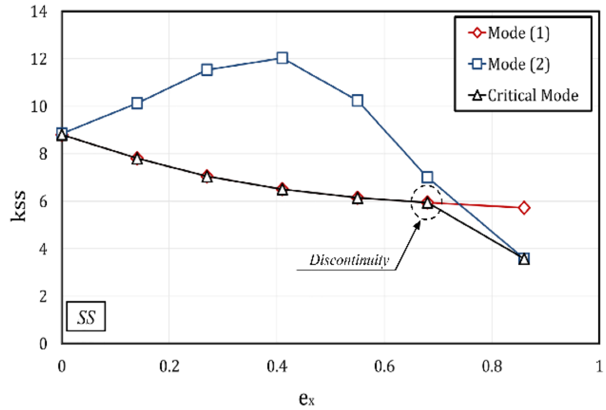

Fig. 14 Buckling coefficient vs. e_x for the plate with $a/L = 0.9$, $H/L = 1.0$, and boundary condition *SS*

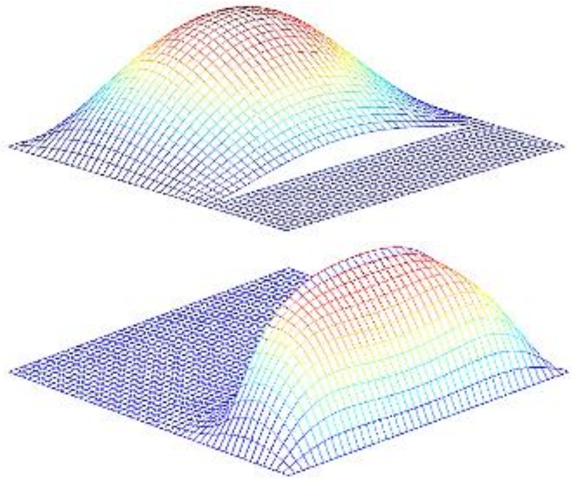

Mode (1) Mode (2)

Fig. 15 First and second buckling mode shapes of a non-centrally cracked plate

drawn in Fig. 14 with a dark line and triangular markers. As seen in the figure, this is a non-smooth curve with a weak discontinuity at a point around $e_x = 0.7$. Such behavior is also observed in cases of some other curves. Investigation of the plate buckling mode shapes can be helpful in explaining this observation.

Fig. 15 shows two probable buckling modes for such a plate, called as mode (1) and mode (2). The non-central crack divides a plate into two non-equal areas. In buckling mode (1), the out-of-plane deformation of the larger area is more visible than that of the small area, while an opposite observation is made in case of mode (2).

The buckling coefficient-crack location curves corresponding to modes (1) and (2) are also shown in Fig. 14 by red and blue lines, respectively. Comparing these curves reveals that the critical buckling coefficient may correspond to either mode (1) or mode (2), depending on the crack location. Therefore, the points on some curves shown in Figs. 7 through 9 may be corresponding to different buckling modes. This finding may justify some disparate trends at various parts of such curves.

8. Conclusions

The objective of this study was to evaluate the effects of various boundary conditions (*SS*, *CS*, and *CC*), aspect ratios (0.5, 1.0, and 2.0), and crack lengths as well as locations on the buckling stability of thin plates under uniaxial compression. Unlike the previous studies which mostly focused on small cracks, the effects of small-, intermediate-, and large-size cracks were investigated in this research endeavor. To this end, a computational code was developed using MATLAB software in order to create numerical models on the basis of singular finite element method. Eigen-buckling analyses were additionally performed for stability assessment of the centrally and non-centrally cracked plates.

This study showed that the buckling capacity of a cracked plate can be highly dependent on the crack parameters, i.e. crack length and location. The degree of effectiveness of these parameters in plates with various aspect ratios and support conditions was found to be significantly different. The effectiveness of the fixity of the plate supports in conjunction with its aspect ratio was also investigated and it was found that cracked plates with small aspect ratios and more fixity in their supporting edges have higher buckling capacity. Overall, based on the findings of this study on the effectiveness of the plate aspect ratio, support conditions, and crack length as well as location on the buckling capacity of cracked plates, careful consideration of all aforementioned influencing parameters in buckling analysis of plates can lead to the efficient stability design and application of such commonly-used, thin-walled members.

References

Agnihotri, G. (1993), "Stress analysis of a crack using the finite element method", *Eng. Fract. Mech.*, **44**(1), 109-125.

Bouchiba, M.S. and Serier, B. (2016), "New optimization method of patch shape to improve the effectiveness of cracked plates repair", *Struct. Eng. Mech.*, **58**(2), 301-326.

Brighenti, R. (2005a), "Buckling of cracked thin-plates under tension or compression", *Thin-Wall. Struct.*, **43**(2), 209-224.

Brighenti, R. (2005b), "Numerical buckling analysis of compressed or tensioned cracked thin plates", *Eng. Struct.*, **27**(2), 265-276.

Ghanbari Ghazijahani, T., Jiao, H. and Holloway, D. (2014), "Experiments on dented steel tubes under bending", *Adv. Struct. Eng.*, **18**(11), 1807-1817.

Ghanbari Ghazijahani, T., Jiao, H. and Holloway, D. (2015), "Plastic buckling of dented steel circular tubes under axial compression: An experimental study", *Thin-Wall. Struct.*, **92**(July), 48-54.

Ghanbari Ghazijahani, T., Showkati, H. and Jiao, H. (2016), "Buckling assessment of dented truncated cones under external pressure", *Adv. Comput. Des.*, **1**(4), 345-356.

Guz, A.N. and Dyshel, M.S. (2001), "Fracture and buckling of thin panels with edge crack in tension", *Theoret. Appl. Fract. Mech.*, **36**(1), 57-60.

Guz, A.N. and Dyshel, M.S. (2002), "Buckling and cracking characteristics of two-layered plate in tension", *Theoret. Appl. Fract. Mech.*, **38**(1), 103-107.

Jamal-Omidi, M., Falah, M. and Taherifar, D. (2014), "3-D fracture analysis of cracked aluminum plates repaired with single and double composite patches using XFEM", *Struct. Eng. Mech.*, **50**(4), 525-539.

Khedmati, M.R., Edalat, P. and Javidruzi, M. (2009), "Sensitivity analysis of the elastic buckling of cracked plate elements under axial compression", *Thin-Wall. Struct.*, **47**(5), 522-536.

Markström, K. and StoÅkers, B. (1980), "Buckling of cracked members under tension", *Int. J. Sol. Struct.*, **16**(3), 217-229.

Pan, Z., Cheng, Y. and Liu, J. (2013), "A semi-analytical analysis of the elastic buckling of cracked thin plates under axial compression using actual non-uniform stress distribution", *Thin-Wall. Struct.*, **73**(December), 229-241.

Reddy, J.N. (2006), *An Introduction to the Finite Element Method*, 3rd Edition, McGraw-Hill Companies Publishing, New York, U.S.A.

Sadek, S.C. and Tawfik, T. (2016), "Buckling of cracked plate reinforced", *Proc. Struct. Integr.*, **1**, 234-241.

Shahverdi, H. and Navardi, M.M. (2017), "Free vibration analysis of cracked thin plates using generalized differential quadrature element method", *Struct. Eng. Mech.*, **62**(3), 345-355.

Seif, A.E. and Kabir, M.Z. (2017), "Experimental study on the fracture capacity and fatigue life reduction of the tensioned cracked plate due to the local buckling", *Eng. Fract. Mech.*, **175**(April), 168-183.

Seifi, R. and Khoda-yari, N. (2011), "Experimental and numerical studies on buckling of cracked thin-plates under full and partial compression edge loading", *Thin-Wall. Struct.*, **49**(12), 1504-1516.

Shaw, D. and Huang, Y.H. (1990), "Buckling behavior of a central cracked thin plate under tension", *Eng. Fract. Mech.*, **35**(6), 1019-1027.

Shi, X.H., Zhang, J. and Soares, C.G. (2017), "Experimental study on collapse of cracked stiffened plate with initial imperfections under compression", *Thin-Wall. Struct.*, **114**(May), 39-51.

Sih, G.C. and Lee, Y.D. (1986), "Tensile and compressive buckling of plates weakened by cracks", *Theoret. Appl. Fract. Mech.*, **6**(2), 129-138.

Stren, M. (1979), "Families of consistent conforming elements with singular derivative fields", *Int. J. Numer. Meth. Eng.*, **14**(3), 409-421.

Timoshenko, S.P. and Gere, J.M. (1961), *Theory of Elastic Stability*, 2nd Ed., McGraw-Hill Book Companies Publishing, New York, NY, USA.

Vafai, A., Javidruzi, M. and Estekanchi, H.E. (2002), "Parametric instability of edge cracked plates", *Thin-Wall. Struct.*, **40**(1), 29-44.

CC

Notation

The following symbols are used in this paper:

a	half crack length
A	area
$[B]$	strain-displacement matrix
$[C]$	transformation matrix (Eq. (5))
D	plate flexural rigidity
e_x	distance between the central y-axis of the

	plate and the crack
E	Young's modulus
H	half plate width
k	plate buckling coefficient
k_{cc}, k_{cs}, k_{ss}	plate buckling coefficients for clamped, clamped-simple, and simple supports
$[K_g]$	geometric stiffness matrix
$[K_s]$	standard stiffness matrix
L	half plate length
N_x, N_{xy}, N_y	in-plane forces per unit length of plate boundary
r	radial coordinate in polar coordinate system
t	plate thickness
U	strain energy due to bending
V	potential energy from external mechanical loads
w	transverse deflection
x, y, z	Cartesian coordinates
$\alpha_1, \ldots, \alpha_9$	constants/unknowns in Eq. (1)
$\{\alpha\}$	vector of constants/unknowns (refer to Eqs. (1) and (2))
$\{\beta_i\}$	plate buckling mode-shape (eigen) vector
$\{\delta_e\}$	nodal degrees of freedom vector
$\{\delta W\}$	vector of virtual variation of lateral displacement of the plate
θ	angular coordinate in polar coordinate system
λ_{cr}	the lowest value of λ_i
λ_i	eigenvalue
ν	Poisson's ratio
Π	total potential energy
$[\varphi]$	interpolation functions matrix (Eq. (3))
$[\Phi]$	shape function matrix (Eq. (7))